MicroRNA-21-5p expression in extracellular vesicles is increased in the blood of aging mice and in vascular endothelial cells induced by ionizing radiation

KEISUKE YAMAMOTO[1] and MITSURU CHIBA[1,2]

[1]Department of Bioscience and Laboratory Medicine, Graduate School of Health Sciences, Hirosaki University, Hirosaki, Aomori 036-8564, Japan; [2]Research Center for Biomedical Sciences, Hirosaki University, Hirosaki, Aomori 036-8564, Japan

Abstract. In recent years, the Japanese population has been aging and the risk of contracting various age-related diseases has increased. Thus, there is a need to analyze components that are characteristic of aging and examine their association with diseases to detect age-related diseases at an early stage. In the present study, microRNAs (miRNAs/miRs) in serum extracellular vesicles (EVs) of 82-102-week-old mice were analyzed to identify miRNAs characteristic of aging. Increased expression of mmu-miR-21a-5p was observed. These miRNAs may be derived from senescent vascular endothelial cells, and RNA-sequencing data (GSE130727) of HUVECs induced to senesce by 4 Gy of radiation revealed that the miRNAs were involved in the cell cycle and DNA repair. Annotations to senescence-related pathways were also identified. Reduced expression of the miR-21-5p target gene, which has an identical sequence in humans and mice, was confirmed. In HUVECs induced to age under similar conditions, increased senescence-associated β-galactosidase activity and increased intracellular miR-21-5p expression were observed. A portion of the miR-21-5p was secreted extracellularly by internalizing tetraspanin-positive EVs, and miR-21-5p was secreted into the extracellular space. The present study also demonstrated that miR-21-5p expression was upregulated and extracellular secretion of miR-21-5p was enhanced during vascular endothelial cell senescence. These findings suggested that increased serum miR-21-5p represents a biomarker for vascular endothelial cell senescence.

Correspondence to: Dr Mitsuru Chiba, Department of Bioscience and Laboratory Medicine, Graduate School of Health Sciences, Hirosaki University, 66-1 Hon-cho, Hirosaki, Aomori 036-8564, Japan
E-mail: mchiba32@hirosaki-u.ac.jp

Introduction

Recently, Japan's population has started aging and the risk of contracting various age-related diseases has increased. Therefore, analyzing component characteristics of aging and examining their relationship with diseases to detect age-related diseases at an early stage is necessary (1). Aging is often accompanied by an increase in lifestyle-related diseases and many other diseases, and early detection of disease is one of the most important issues, especially in maintaining a healthy life expectancy.

At the cell level, senescence is a state in which cells cease to divide and undergo distinctive phenotypic changes, including altered gene expression and the secretion of senescence-associated secretory phenotype (SASP) factors (2). SASP has profound effects, not only on the senescence cells themselves, but also on the surrounding tissue microenvironment to promote inflammation, tissue dysfunction, and progression of aging- and senescence-related diseases (3,4). Cellular senescence may be readily induced by repeated passage of cultured cells or irradiation (5,6).

Recently, extracellular vesicles (EVs), such as exosomes, have been reported to be involved in the onset and progression of aging and aging-related diseases (7). EVs are small particles released from cells that contain DNA, RNA, proteins, and lipids (8,9). They may serve as useful biomarkers for various diseases because they reflect the physiological state of the releasing cells (10-12). miRNAs (microRNAs) are known to be abundant among the various RNAs contained in EVs (13). miRNAs are approximately 21-24 nucleotides in length and are small noncoding RNAs that bind to target mRNAs and either suppress translation or promote mRNA degradation to post-transcriptionally regulate gene expression (14). The role of miRNAs in cellular senescence has been shown to influence many biological processes associated with aging, including cell proliferation, apoptosis, and the inflammatory response (15,16). For example, miR-125b, miR-504, miR-25, and miR-30d directly act on p53 and suppress its function (17). miR-21-5p is a small noncoding RNA that was first reported as an miRNA in cancer-related studies (18). It has been reported that miR-21 increases with age in the heart of mice (19). It reportedly inhibits cell cycle progression via CDC25A (20).

EVs are abundant in body fluids, such as blood, and they are secreted by various cells throughout the body and are present in body fluids in a mixed state (21). Blood is in constant contact with vascular endothelial cells, and it is believed that EVs-derived from vascular endothelial cells are abundant in the blood (22,23). RNA-sequencing analysis of endothelial cells and fibroblasts induced into senescence by irradiation revealed gene expression changes when senescence is induced, including senescence-specific gene expression patterns (24). However, the relationship between changes in the expression of blood miRNAs and vascular endothelial cell senescence has not been examined.

In this study, we examined the characteristics of serum miRNA expression in aging mice and the expression of miRNAs inside and outside the cells of senescence-induced vascular endothelial cells. Our results provide insight into senescence-induced and secreted miRNAs in vascular endothelial cells.

Materials and methods

Mice and blood collection. C57BL6NJcl male mice were purchased from CLEA Japan. They were acclimated for at least one week before initiating the experiments. The mice were provided a solid diet of CE2 (CLEA Japan) and water *ad libitum* and were housed in a conventional animal room with 12 h light/dark cycles at room temperature and 40-50% humidity. The mice were housed up to 5 mice per cage containing bedding, feed, and water, which were changed weekly. The mice were observed 2-3 times/day for monitoring. No abnormalities in mouse health or behavior were observed. Five 8-week-old mice were designated 'Young' mice, and five 82-week-old and three 102-week-old mice were designated 'Aging' mice. Small animal anesthesia machines (Muromachi Kikai) were used to anesthetize the mice. Isoflurane vaporized to a concentration of 4-5% was administered to the mice and maintained at 2-3% throughout the experiment. Following anesthesia, approximately 0.5-1.0 ml of blood was drawn from the heart, and the mice were promptly cervically dislocated to minimize distress. The time from the beginning of anesthesia to the end of blood collection was less than 10 min per animal. Death was confirmed by respiratory and cardiac arrest. Blood was placed in a Microtainer (cat. no. 365967, Becton Dickinson) for serum separation. After checking for coagulation, the blood was centrifuged at 6,000 x g for 3 min. The serum was separated and stored at -80°C until use. The experiment was approved by the Hirosaki University Animal Experiment Ethics Committee and conducted based on the Hirosaki University Animal Experiment Guidelines (Approval No. AE01-2023-097-1).

Serum RNA extraction. The serum was filtered through a 0.20 μm filter and the RNAs derived from EVs were extracted from 200 μl of serum using the exoRNeasy midi kit (cat. no. 77144, Qiagen) and cel-miR-39 was added as a spike-in RNA. The concentration of the extracted EV-derived RNAs was measured using a Qubit™ microRNA Assay Kit (cat. no. Q32880, ThermoFisher Scientific) and a Qubit 4 Fluorometer (cat. no. Q33238, ThermoFisher Q33238, ThermoFisher Scientific) based on the manufacturer's protocol.

To confirm the size of the RNAs in the serum EVs, an Agilent 2100 Bioanalyzer (Agilent Technologies, Inc.) and the Agilent RNA 6000 Pico kit (cat. no. 5067-1513, Agilent Technologies, Inc.) were used to perform RNA electrophoresis based on the manufacturer's protocol.

miRNA microarray. To examine miRNA expression in mouse serum, a miRNA microarray analysis was performed using 1.8 ng of RNAs extracted by the method described above. Microarray analysis was performed as previously described according to the manufacturer's instructions (25,26). The miRNA Complete Labeling Reagent and Hyb kit (cat. no. 5190-0456, Agilent Technologies) was used to label mouse serum EVs-derived RNAs with Cyanine-3 and hybridized to SurePrint G3 Mouse 8x60 K miRNA microarray slides (version 21.0) (cat. no. G4872A, design ID: 070155, Agilent Technologies) at 55°C for 20 h. The fluorescence signals were detected using a SureScan Microarray Scanner (Agilent Technologies) and quantified using Feature Extraction software (Agilent Technologies). The microarray data were analyzed using R (version 4.3.1) and quantile normalization was done using limma (27). Microarray data were analyzed for genes with a fold-change cutoff of ≥1.5 (28,29), as the commonly used cutoff in various studies detecting genes in aging mice compared with young mice. A t-test was performed to identify genes with P-values <0.05. The resulting microarray data were registered to Gene Expression Omnibus (GSE274943).

Reverse transcription-quantitative PCR (RT-qPCR) of serum EV miRNAs. RT-qPCR was used to validate the miRNAs in mouse serum. Total RNA and reverse transcriptase were incubated at 37°C for 1 h for cDNA synthesis. Then, qPCR was performed using 10-fold diluted cDNA, TB Green Advantage qPCR Premix (cat. no. 639676, Takara Bio), and miRNA-specific primers (Table SI) based on the manufacturer's protocol. The conditions for qPCR were as follows: cDNA was denatured at 95°C for 10 sec in a total volume of 25 μl, followed by 40 cycles of 95°C for 5 sec and 60°C for 20 sec. The cDNA was then incubated at 95°C for 5 sec and 60°C for 20 sec for 40 cycles. Cel-miR-39 was used as an external control. The quantitation of gene expression was done using the $2^{-\Delta\Delta Cq}$ method (30).

Reanalysis of RNA-sequence data. To evaluate gene expression in senescence-induced HUVECs, RNA-sequence data of HUVECs exposed to 4 Gy of radiation for 10 days were downloaded from the Sequence Read Archive (SRA) (GSE130727, SRR9016151-SRR 9016156). FASTQ files downloaded from SRA were quality-checked and trimmed using Fastp (31). Gene expression levels were calculated from FASTQ files using salmon (32) and tximport (33). R (version 4.3.1) was used for data analysis and quasi-likelihood F-tests were used with the expression analysis packages, limma (27) and edgeR (34). The p-values for multiple correction by the Benjamini-Hochberg method were less than 0.05. In addition, genes with a fold-change ≥1.5 are selected. Hierarchical clustering and principal component analysis (PCA) were done to examine differences in gene expression between the 4 Gy-irradiated and unirradiated HUVECs. Gene Set Enrichment Analysis (GSEA) and Gene Ontology (GO) analysis were performed using ClusterProfiler (35), fgsea, and

the AnnotationDbi package. Kyoto Encyclopedia of Genes and Genomes (KEGG) and pathway analysis using ReactomePA were also conducted (36).

Cell culture. HUVECs, single donor P1 (cat. no. C-12200, Promo Cell) were purchased from Takara Bio, and cultured in Basic Cell Growth Medium 2 Kit (cat. no. C-22011, Promo Cell) with 5% Fetal Calf Serum (FCS), 5.0 ng/ml Epidermal Growth Factor (recombinant human), 10 ng/ml Basic Fibroblast Growth Factor (recombinant human), 10 ng/ml Insulin-like Growth Factor (Long-type), 20 ng/ml Insulin-like Growth Factor (Long R3 IGF, recombinant human), 1.0 μg/ml ascorbic acid, 22.5 μg/ml heparin, and 0.2 μg/ml hydrocortisone. For the recovery of EVs, exosome-depleted fetal bovine serum (cat. no. 558-39501, Fujifilm Wako) was used instead of FCS in the above medium. 41220, Promo Cell) to pass the HUVECs.

X-ray irradiation. HUVECs from P2 to P6 were seeded at $1x10^5$ cells/60 mm dish and incubated overnight at 37˚C in a 5% CO_2 atmosphere. HUVECs were irradiated with 4 Gy X-rays (MBR-1520R-3 X-ray machine, Hitachi Ltd.) at a dose rate of 1.0 Gy/min (150 kVp, 20 mA, 0.5 mm aluminum, and 0.3 mm copper filters).

RNA extraction from HUVECs. Total RNA was extracted from HUVECs that were cultured for 10 days after 4 Gy irradiation. The control group consisted of HUVECs that were passaged on day 5 and cultured for 10 days to avoid becoming 100% confluent. Intracellular RNA was extracted from cell pellets after centrifuging at 300 g for 3 min using the miRNeasy mini kit (cat. no. 217004, Qiagen) based on the manufacturer's protocol. The concentration of the extracted RNA was measured using a Nanodrop instrument (ThermoFisher Scientific) based on the manufacturer's protocol.

The HUVEC culture supernatant was filtered through a 0.20 μm filter and RNAs from the EVs were extracted from 2 ml of culture supernatant using the exoRNeasy midi kit (cat. no. 77144, Qiagen). The concentration of RNAs in the extracted EVs was determined using the Qubit™ microRNA Assay Kit (cat. no. Q32880, ThermoFisher Scientific) and Qubit 4 Fluorometer (cat. no. Q33238, ThermoFisher Scientific) based on the manufacturer's protocol.

RT-qPCR from HUVECs. RT-qPCR was performed to confirm the expression change of miR-21-5p in HUVECs cultured for 10 days after 4 Gy irradiation. Total RNA was reverse-transcribed into cDNA at 37˚C for 1 h. qPCR was performed with 10-fold diluted cDNA using the TB Green Advantage qPCR Premix (cat. no. 639676, Takara Bio) and miRNA-specific primers (Table SI) based on the manufacturer's protocol. U6 small nuclear RNA was used as an internal control. In the Mir-X miRNA First-Strand Synthesis kit (cat. no. 638313, Takara Bio) containing the U6 primer, the U6 primer sequence is a trade secret and not disclosed.

RT-qPCR was used to validate the messenger RNAs (mRNAs) of the candidate miR-21-5p target genes and genes that were downregulated by RNA-sequencing reanalysis in HUVECs cultured for 10 days following 4 Gy irradiation. Candidate target genes were downloaded from TargetScan (https://www.targetscan.org/vert_72/). cDNA synthesis was done using 200 ng of total RNA extracted from HUVECs cultured for 10 days after 4 Gy irradiation with the High Capacity cDNA Reverse Transcriptase Kit (cat. no. 4368814, ThermoFisher Scientific) based on the manufacturer's protocol. Total RNA (200 ng) and 2x Reverse Transcriptase Master Mix solution were mixed in a total volume of 20 μl. The reverse transcription reaction was performed at 25˚C for 10 min, 37˚C for 120 min, and 85˚C for 5 min. Next, qPCR was done using 5-fold diluted cDNA, Power SYBR Green PCR Master Mix (2x) (cat. no. 4367659, ThermoFisher Scientific), and gene-specific primer pairs (Table I) based on the manufacturer's protocol. Of the primers used, primer 3 (version 4.1.0) was designed for RT-qPCR of mRNA. Actin beta was used as an internal control.

RT-qPCR was performed for changes in the expression of miR-21-5p in EVs in culture supernatants secreted from HUVECs cultured for 10 days after 4 Gy irradiation. Total RNA (100 μg) was extracted from EVs in the culture supernatants secreted from HUVECs 10 days after 4 Gy irradiation. The Mir-X miRNA First-Strand Synthesis kit (cat. no. 638313, Takara Bio) was used for cDNA synthesis based on the manufacturer's protocol. Total RNA and reverse transcriptase were incubated at 37˚C for 1 h. Then, qPCR was performed using 10-fold diluted cDNA using TB Green Advantage qPCR Premix (cat. no. 639676, Takara Bio) and miRNA-specific primers (Table SI) based on the manufacturer's protocol. The respective miRNA sequences published on miRbase were used as primer sequences. Cel-miR-39 was used as an external control. The quantitation of gene expression was done using the $2^{-\Delta\Delta Cq}$ method (30).

Senescence-associated β-galactosidase (SA-β-GAL) staining. To detect cell senescence in HUVECs cultured for 10 days following 4 Gy irradiation, the senescence β-galactosidase staining kit (cat. no. 9860, Cell Signaling Technology) was used. HUVECs ($1x10^5$ cells) were treated with 1x Fixative Solution. After washing three times with phosphate-buffered saline (PBS), 1.0 ml of β-galactosidase stain was added and incubated at 37˚C overnight. HUVECs were observed under an optical microscope with the β-galactosidase staining solution remaining.

To quantify cellular senescence in HUVECs, the cellular senescence detection kit SPiDER-βGal (cat. no. SG02, Dojindo Molecular Technologies, Inc.) was used. HUVECs ($1x10^5$ cells) were collected and incubated with Hank's Balanced Salt Solution (HBSS). After washing twice with HBSS, 1.0 ml of the prepared SPiDER-βGal working solution was added and incubated in a 5% CO_2 incubator at 37˚C for 1 h. After washing twice with HBSS, 1.0 ml of the prepared SPiDER-βGal working solution was added and incubated at 37˚C in a 5% CO_2 incubator for 30 min. The supernatant was removed by aspiration, the cells were washed twice with HBSS, and detached with the DetachKit (cat. No. C-41220, Promo Cell). The fluorescence of the detached HUVECs was analyzed using CytoFLEX flow cytometer and CytExpert software version 2.4 (both Beckman Coulter) and kaluza2.2 software (Beckman Coulter).

Cell cycle analysis. To confirm the cell cycle of 4 Gy-irradiated and nonirradiated HUVECs, each exfoliated cell was fixed

Table I. Primer pairs for reverse transcription-quantitative PCR.

Primer name	Sequence (5'-3')	Amplicon size, bp
CDC25A forward	CTACTGATGGCAAGCGTGTC	88
CDC25A reverse	TCTCTCTCACATACCGGCAC	
MSH2 forward	CATGTCACAGCACTCACCAC	99
MSH2 reverse	GCTCTGCAACATGAATCCCA	
MTAP forward	TTCTTGTGCCAGAGGAGTGT	102
MTAP reverse	CACCGGAGTCCTAGCTTCTT	
MTHFD1 forward	AAAGAGAGGGCGAGCTTCAT	97
MTHFD1 reverse	AACGCTTGGCACTCTCTACT	
ZNF367 forward	CACATCAGCGTCTTCACACC	83
ZNF367 reverse	CGGTTTGCATGGGTGAATCT	
ZNF704 forward	CTCGCTCCATCTGTCTCCTT	116
ZNF704 reverse	CATTGCTGCTGTCACCTTGT	
ACTB forward	CCAACCGCGAGAAGATGA	97
ACTB reverse	CCAGAGGCGTACAGGGATAG	

ACTB, actin β; *CDC25A*, cell division cycle 25A; *MSH2*, mutS homolog 2; *MTAP*, methylthioadenosine phosphorylase; *MTHFD1*, methylenetetrahydrofolate dehydrogenase cyclohydrolase and formyltetrahydrofolate synthetase 1; *ZNF367*, zinc finger protein 367; *ZNF704*, zinc finger protein 704.

by adding 70% ethanol and incubated at -20°C overnight or longer. Then, each exfoliated cell was washed three times with PBS, and 200 μl of 250 μg/ml RNase A (cat. no. 318-06391, Fujifilm Wako) was added and incubated at room temperature for 30 min. Propidium iodide was then added at 50 μg/ml and fluorescence was detected with a CytoFLEX flow cytometer and CytExpert software version 2.4 (both Beckman Coulter). All events were measured up to 10,000 events per sample. For data analysis, histograms were generated using kaluza2.2 software (Beckman Coulter).

Detection of EV markers. HUVEC culture supernatant (2 ml) was centrifuged at 300 g for 3 min. The collected supernatant was passed through a 0.20 μm filter and enriched for EVs by ultrafiltration using an Amicon Ultra 0.5 ml centrifugal filter (cat. No. UFC510096, Merke Millipore). EVs were then collected using the PS capture™ Exosome Flow Cytometry Kit (cat. no. 297-79701, Fujifilm Wako) based on the manufacturer's recommended protocol. Fluorescein isothiocyanate (FITC) anti-human CD63 Antibody (cat. no. 353005 BioLegend), FITC anti-human CD9 Antibody (cat. no. 312103, BioLegend), FITC anti-human CD81 Antibody (cat. no. 349503, BioLegend), and FITC Mouse IgG1, κ isotype Ctrl antibody (cat. no. 400110, BioLegend) were used. The data were analyzed using a CytoFLEX flow cytometer and CytExpert software version 2.4 (both Beckman Coulter). For data analysis, histograms were generated using kaluza2.2 software (Beckman Coulter).

Statistical analysis. All statistical analyses were performed using R (version 4.3.1). Two-group tests were subject to the Shapiro-Wilk test to confirm normality, followed by the F test, and Welch's T-test for data without equal variance. Mann-Whitney's U test was performed if normality was rejected. The significance level was set at $P<0.05$. For all experiments using HUVECs, the number of samples was n=4.

Results

Expression of blood EV mmu-miR-21a-5p is increased in aging mice. In our previous study, we found that cognitive function was impaired in 58-week-old mice in the Morris water maze (28). To further confirm changes in the expression of miRNAs in blood EVs in aged mice, we compared EVs RNAs from 'Aging' (82 and 102 weeks old) and 'Young' (8 weeks old) mice. The size of the EV RNA in the serum of the Aging and Young mice was found to be in the range of 25-200 nucleotides (nt) (Fig. 1A). We performed a mouse miRNA microarray using the extracted serum RNAs to identify miRNAs whose expression was significantly altered in Aging mice compared with Young mice. We found that mmu-miR-21a-5p, mmu-miR-3473b, and mmu-miR-7047-5p were significantly increased in the serum of the Aging mice (Fig. 1B). RT-qPCR was used to confirm the expression of the three miRNAs that were significantly increased. We found that mmu-miR-21a-5p and mmu-miR-7047-5p were significantly increased in Aging mice (Fig. 1C). This suggests that these two blood miRNAs are molecules associated with aging. One possible reason for the discrepancy between PCR results and microarray results is that microarrays and RT-qPCR have different sensitivities, so a sample that is statistically significant by microarray may not be statistically significant by RT-qPCR.

Differentially expressed genes in HUVECs irradiated with 4 Gy. The altered miRNAs described above may be derived from the senescence of vascular endothelial cells (22,23). Therefore, we considered the possibility that the senescence of vascular endothelial cells affects the expression of miRNAs in
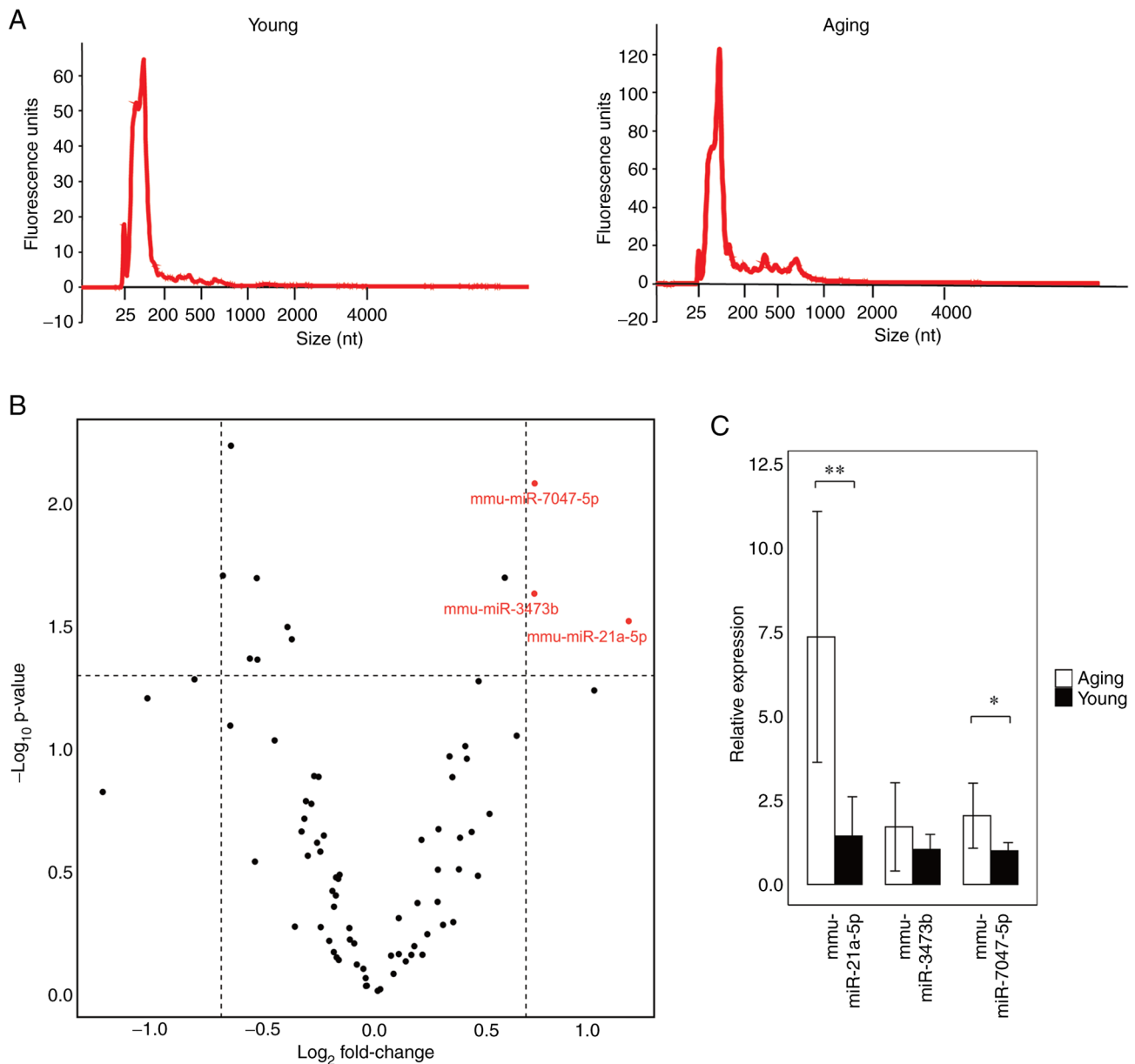
Figure 1. miRNA microarray analysis of blood EVs in aging and young mice. RNA of EVs in the serum of aging and young mice was extracted for miRNA expression analysis. The exoRNeasy midi kit was used to extract EV RNA. (A) Confirmation of serum EV RNA size in aging and young mice. The size of extracted EV RNA was confirmed using an Agilent RNA 6000 Pico kit. Small RNA of 25-200 nt was observed in the serum RNA of both aging and young mice. (B) Expression analysis of serum EV miRNAs in aging and young mice. miRNAs with ≥1.5-fold expression change and P<0.05 in aging mice compared with young mice were examined. The mmu-miR-21a-5p, mmu-miR-3473b and mmu-miR-7047-5p transcripts were detected in the volcano plot. (C) RT-qPCR validation of miRNAs identified in the volcano plot. RT-qPCR validation was performed for the three miRNAs verified to be increased in (B). In the serum of the aging mice, mmu-miR-3473b was increased; however, this was not statistically significant, whereas mmu-miR-21a-5p and mmu-miR-7047-5p were statistically significantly increased. *P<0.05. **P<0.01. EV, extracellular vesicle; miRNA/miR, microRNA; RT-qPCR, reverse transcription-quantitative PCR.

blood EVs. To confirm the gene expression changes in senescence-induced HUVECs, we downloaded and reanalyzed the RNA-sequence data (GSE130727, SRR9016151-SRR9016156) of 4 Gy-exposed HUVECs. Cluster analysis revealed that gene expression was different between 4 Gy-irradiated and nonirradiated HUVECs (Fig. 2A). Similarly, PCA showed a significant change in gene expression between the 4 Gy-irradiated and nonirradiated HUVECs (Fig. 2B). Furthermore, differentially expressed gene (DEG) analysis using edgeR identified 1881 genes that were altered by ≥1.5-fold (Fig. 2C). This reanalysis indicated that 4 Gy irradiation alters the expression of many HUVEC genes.

4 Gy irradiation induces changes in the expression of genes involved in cell division and cell cycle in HUVECs. Enrichment analysis was performed on 1881 genes that were altered by DEG analysis of the RNA sequences. A GSEA analysis was performed on the GO terms to determine whether senescence induction of HUVECs by 4 Gy irradiation was affected by a decrease or increase of the altered genes. The results indicated that most of the variable genes were enriched in the downregulated gene group because the enrichment score was less than zero (Fig. 3A). Based on this result, GO enrichment analysis was performed on the downregulated genes, and terms associated with DNA replication and cell division
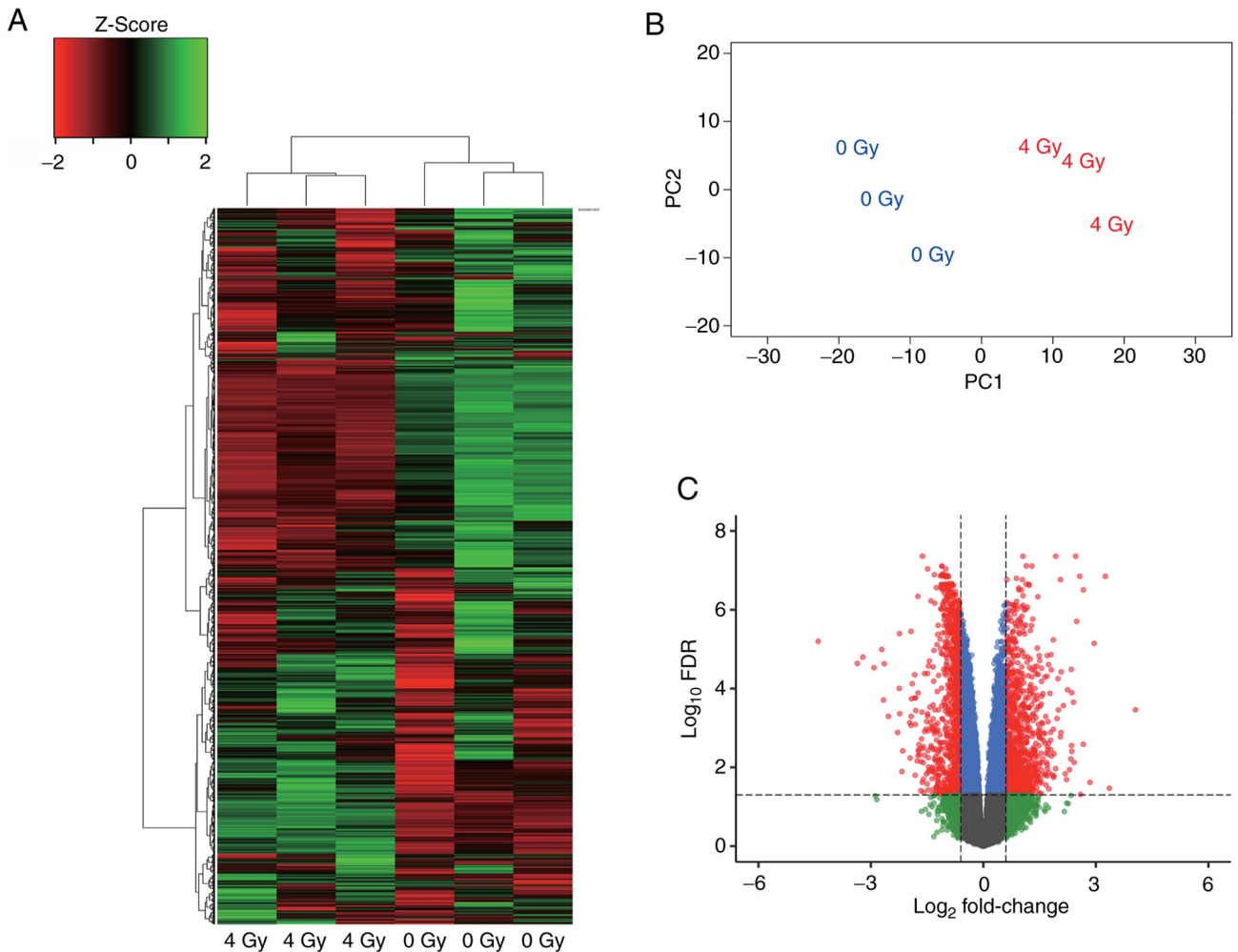
Figure 2. RNA-sequencing reanalysis of HUVECs irradiated with 4 Gy. To examine gene expression in 4 Gy-irradiated and senescence-induced HUVECs, the RNA-sequencing data from GSE130727 (SRR9016151 to SRR9016156) were reanalyzed. (A) Heat map showing hierarchical clustering of the gene expression profiles of 4 Gy-irradiated HUVECs (4 Gy) and nonirradiated HUVECs (0 Gy). Each row represents a gene and each column represents a sample. Gene expression levels were normalized, with green indicating upregulation and red indicating downregulation. (B) PCA plot showing the distribution of 4 Gy-irradiated (red) and nonirradiated (blue) HUVECs. PC1 and PC2 accounted for 79.92 and 14.27% of the total variance, respectively. Each point represents an individual sample. (C) Volcano plot of the differentially expressed genes in 4 Gy-irradiated and nonirradiated HUVECs. Genes with a FDR <0.05 and a fold-change ≥1.5 are plotted in red. FDR, false discovery rate; PC, principal component; PCA, principal component analysis.

were identified (Fig. 3B). In addition, KEGG pathway and Reactome pathway enrichment analyses were also performed and pathways related to the cell cycle and DNA repair were annotated (Fig. 3C and D). These results suggest that there are changes in DNA replication and cell cycle-related genes in 4 Gy-irradiated senescence-induced HUVECs.

Senescence-induced HUVECs cause decreased expression of 6 genes, a miR-21-5p target gene, and change the rate of cell cycle. We identified mmu-miR-21a-5p and mmu-miR-7047-5p as miRNAs that are significantly up-regulated in Aging mice (Fig. 1); however, because no miRNA corresponding to mmu-miR-7047-5p was found in humans, we focused only on miR-21-5p in this study. The results of an RNA-sequence enrichment analysis showed that the expression of 435 genes was decreased by 4 Gy irradiation. The common genes among the 378 candidate target genes of miR-21-5p were examined by target scan, and cell division cycle 25A (*CDC25A*), mutS homolog 2 (*MSH2*), methylthioadenosine phosphorylase (*MTAP*), methylenetetrahydrofolate dehydrogenase,

cyclohydrolase and formyltetrahydrofolate synthetase 1 (*MTHFD1*), zinc finger protein 367 (*ZNF367*), and zinc finger protein 704 (*ZNF704*) were identified (Fig. 4A). Next, to induce senescence in HUVECs, the cells were cultured for 10 days after 4 Gy irradiation. Total RNA was extracted from the HUVECs for RT-qPCR of intracellular miR-21-5p and the candidate target genes. The results indicated that 4 Gy irradiation increased miR-21-5p expression in HUVECs and decreased the expression of five of the six target candidate mRNAs (Fig. 4B and C). Next, SA-β-GAL staining of 4 Gy-irradiated HUVECs revealed that the cytoplasm of 4 Gy-irradiated HUVECs was stained darker and bluer compared with that of nonirradiated HUVECs (Fig. 4D). To quantitate the staining results, HUVECs were fluorescently stained using the cell senescence detection kit SPiDER-βGal, and the fluorescence intensity was measured by flow cytometry. The average SA-β-GAL fluorescence intensity of nonirradiated HUVECs was approximately 59,000, whereas the average SA-β-GAL fluorescence intensity of 4 Gy-irradiated HUVECs was approximately 150,000, which is a statistically
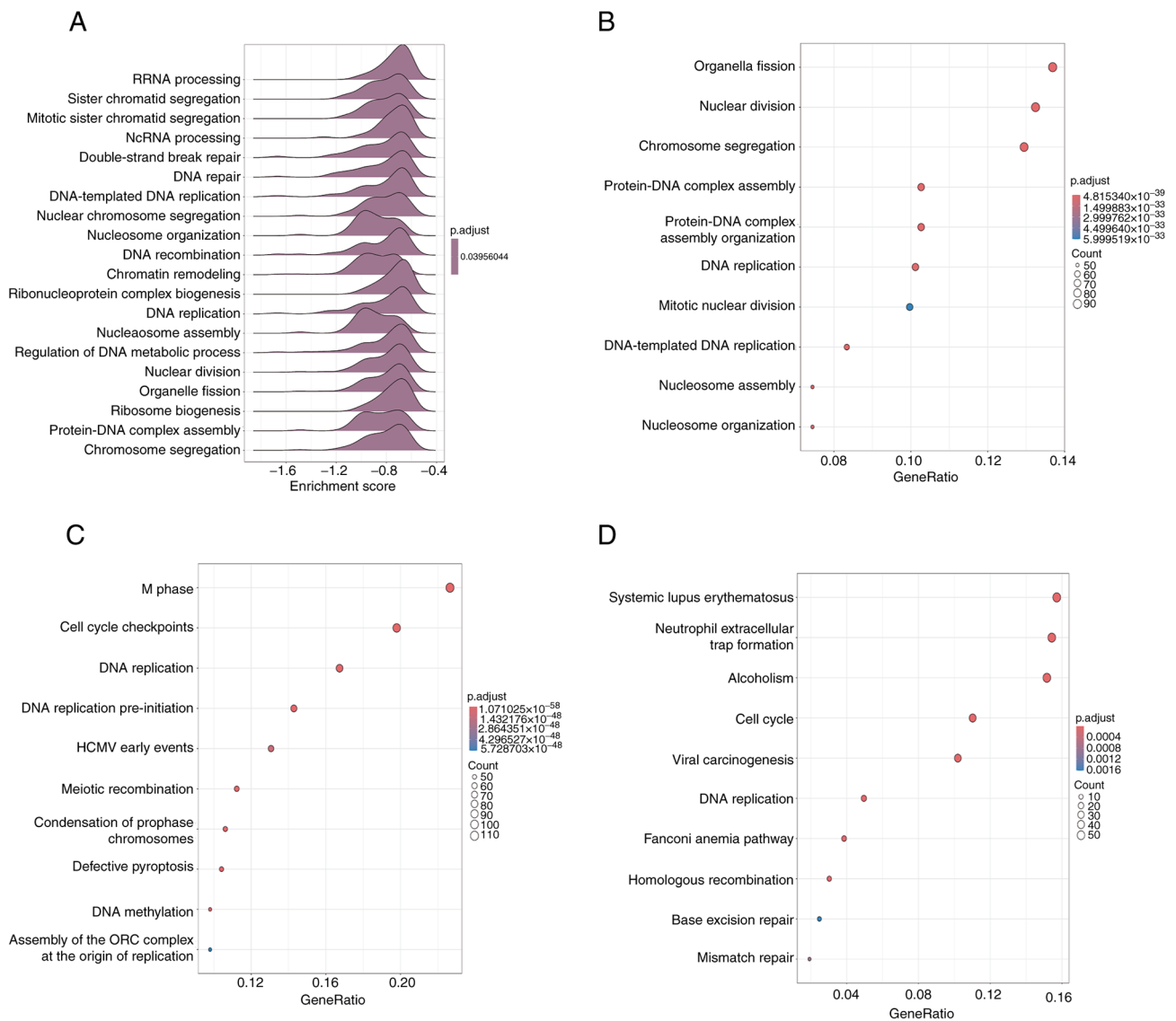
Figure 3. Enrichment analysis of DEGs identified from the RNA-sequencing reanalysis results. (A) Gene Set Enrichment Analysis of DEGs annotated with GO terms. The horizontal axis indicates the enrichment score, and the vertical axis represents the GO terms associated with each annotated gene. (B) Dot plots showing the most significantly enriched GO terms for all gene ontologies. The horizontal axis indicates the GeneRatio and the vertical axis indicates the GO term. The size of the dots represents the number of genes associated with each term and the color indicates the significance of enrichment. (C) Dot plot showing the most significant annotated pathways among all KEGG pathways. The horizontal axis indicates the GeneRatio and the vertical axis indicates the KEGG pathway. The size of the dots represents the number of genes associated with each term and the color indicates the significance of enrichment. (D) Dot plot showing the most significant annotated pathways among the Reactome pathways. The horizontal axis indicates the GeneRatio and the vertical axis indicates the Reactome pathway. The size of the dots represents the number of genes associated with each term and the color indicates the significance of enrichment. DEG, differentially expressed gene; GO, Gene Ontology; HCMV, human cytomegalovirus; KEGG, Kyoto Encyclopedia of Genes and Genomes; ncRNA, non-coding RNA; ORC, origin recognition complex; p.adjust, adjusted P-value; rRNA, ribosomal RNA.

substantial increase (Figs. 4E and S1). Because the expression of *CDC25A*, which is involved in the cell cycle, was decreased, we analyzed the cell cycle of HUVECs cultured for 10 days after 4 Gy irradiation. There were fewer S-phase cells in the 4 Gy-irradiated group compared with that in the nonirradiated group (Figs. 4F and S2). This suggests that 4 Gy irradiation induces senescence in HUVECs and affects the S phase of the cell cycle through increased expression of miR-21-5p.

miR-21-5p expression is increased in EVs secreted from 4 Gy-irradiated HUVECs. To identify tetraspanins, which are surface antigens of EVs secreted from HUVECs cultured for 10 days after 4 Gy irradiation, EVs were collected from 2 ml of culture supernatant using PS capture and incubated with specific antibodies for each FITC-labeled tetraspanin family member and fluorescence was detected by flow cytometry. The results indicated that CD9 was strongly expressed in EVs secreted from HUVECs, confirming that EVs were collected (Fig. 5A). Next, we measured the expression of miR-21-5p in the EVs. The miR-21-5p expression in the supernatant of HUVECs cultured for 10 days after 4 Gy irradiation considerably increased by 2.7-fold compared with the nonirradiated HUVECs (Fig. 5B). This indicates that miR-21-5p is increased not only present intracellularly, but also in EVs of HUVECs irradiated with 4 Gy.
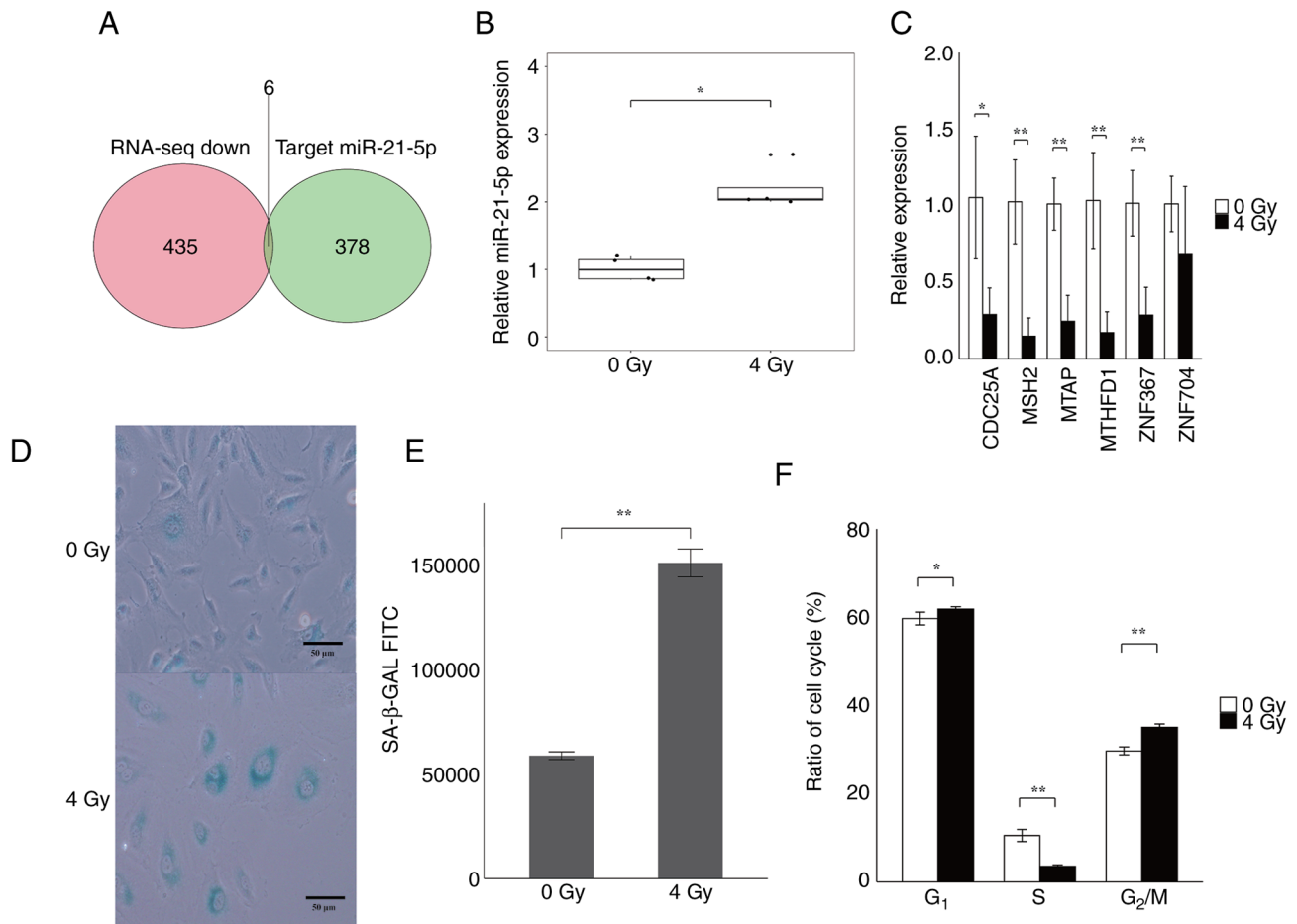
Figure 4. Quantitation of gene expression and cell cycle analysis of senescence-induced HUVECs. Total RNA was extracted from HUVECs cultured for 10 days after 4 Gy irradiation and the expression levels of miR-21-5p and candidate target genes were quantified by RT-qPCR. Senescence and cell cycle analysis of HUVECs was performed. (A) Venn diagram of downregulated genes and miR-21-5p target candidate genes based on the RNA-sequencing reanalysis data. Candidate target genes were downloaded from TargetScan (https://www.targetscan.org/vert_72/). A total of six common genes, including *CDC25A*, *MSH2*, *MTAP*, *MTHFD1*, *ZNF367* and *ZNF704*, were detected. (B) Quantitation of gene expression by RT-qPCR of intracellular miR-21-5p in HUVECs cultured for 10 days following 4 Gy irradiation. The expression of intracellular miR-21-5p was significantly increased in 4 Gy-irradiated HUVECs compared with in nonirradiated HUVECs. (C) Quantitation of targeted-candidate genes in the RNA-sequencing reanalysis data by RT-qPCR. The expression of five genes was significantly decreased in 4 Gy-irradiated HUVECs compared with nonirradiated HUVECs. (D) SA-β-GAL staining of HUVECs cultured for 10 days after 4 Gy irradiation or nonirradiated cells. Blue-stained cells are SA-β-GAL-positive cells. Scale bar, 50 μm. (E) Quantitative analysis of fluorescence intensity by flow cytometry using SPiDER-βGal. The fluorescence intensity was significantly increased in HUVECs irradiated with 4 Gy compared with nonirradiated HUVECs. (F) Cell cycle analysis of HUVECs cultured for 10 days after irradiation with 4 Gy vs. nonirradiated cells. The y-axis indicates the percentage of each cell cycle phase. The 4 Gy-irradiated HUVECs exhibited a significantly lower percentage of S phase cells, and a significant increase in G_1 and G_2/M phase cells compared with non-irradiated HUVECs. All experiments were performed with n=4. *P<0.05, **P<0.01. *CDC25A*, cell division cycle 25A; miR, microRNA; *MSH2*, mutS homolog 2; *MTAP*, methylthioadenosine phosphorylase; *MTHFD1*, methylenetetrahydrofolate dehydrogenase cyclohydrolase and formyltetrahydrofolate synthetase 1; RNA-seq, RNA sequencing; RT-qPCR, reverse transcription-quantitative PCR; SA-β-GAL, senescence-associated β-galactosidase; *ZNF367*, zinc finger protein 367; *ZNF704*, zinc finger protein 704.

Discussion

In this study, we found that mmu-miR-21a-5p was increased in blood EVs of aging mice. Increased expression of miR-21-5p, with the same sequence as that in mice, was observed in senescent HUVECs. Moreover, miR-21-5p was also increased in EVs in the culture supernatant of senescence-induced HUVECs. Based on these findings, the increased expression of EV miR-21-5p extracellularly in senescence-induced HUVECs in vitro suggests increased expression of miR-21-5p in the blood EVs of aging mice. Therefore, increased serum miR-21-5p may be a biomarker for vascular endothelial cell senescence.

Reanalysis of RNA-sequence data from HUVECs identified 1881 genes with altered expression (Fig. 2C). Enrichment analysis of these altered genes revealed that many of the downregulated genes in 4 Gy-irradiated HUVECs were associated with the cell cycle and DNA repair, suggesting that the downregulation of these genes may directly affect these processes. Bouten *et al* (29) performed RNA-sequencing on human lung microvascular endothelial cells irradiated with 10 Gy. In their enrichment analysis, GO term and KEGG pathways also identified terms or pathways related to the cell cycle and DNA repair, which supports our reanalysis of the GSE130727 data (Fig. 3). These molecular changes are thought to result in the inability of cells to proliferate due to reduced expression of genes related to DNA replication and the cell cycle, resulting in cell senescence.

MSH2 is probably involved in processing biologically substantial clustered DNA damages and in executing apoptosis induced by ionizing radiation. The human DNA mismatch
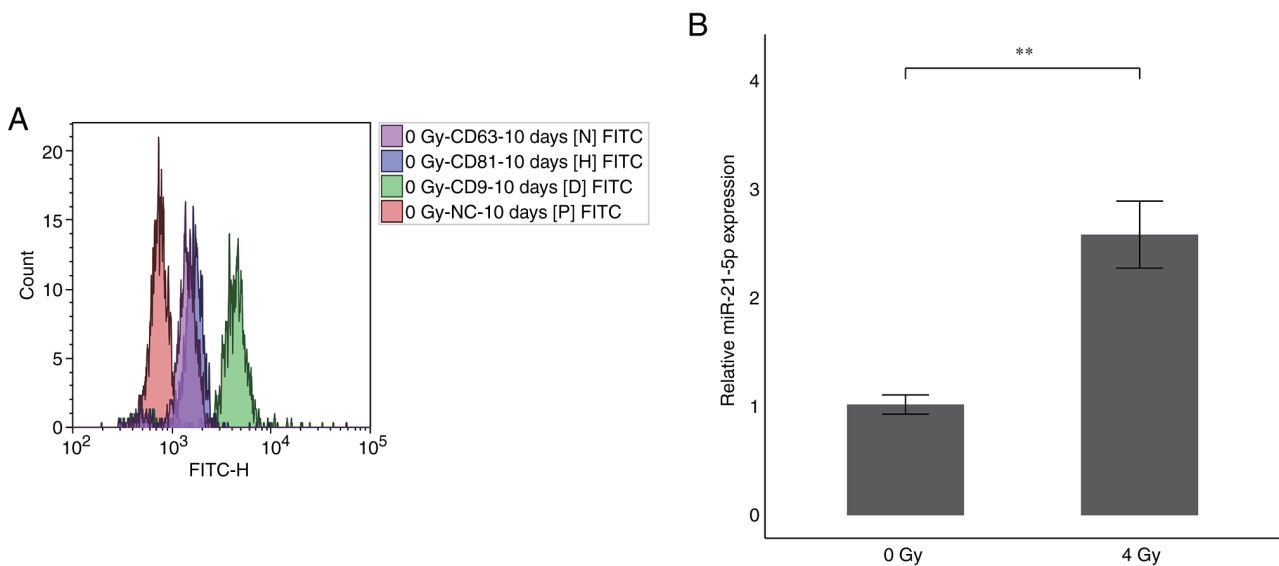
Figure 5. Expression analysis of EV miR-21-5p secreted from HUVECs. Culture supernatants from HUVECs were collected and PS capture was used to confirm the expression of tetraspanins as EV markers and changes in miR-21-5p expression. (A) Expression analysis of tetraspanins CD63, CD9 and CD81 in EVs isolated from HUVEC culture supernatants. Data analysis using Kaluza 2.2 software revealed that CD9 was the most highly expressed tetraspanin in EVs secreted by HUVECs compared with CD63 and CD81. (B) Changes in miR-21-5p expression of EVs from irradiated HUVEC culture supernatants. miR-21-5p expression in EVs from culture supernatants of HUVECs irradiated with 4 Gy and cultured for 10 days was analyzed by RT-qPCR using an exoRNeasy mini kit, and compared with that in non-irradiated controls. qPCR was used and Cel-miR-39 was used as an external control. Expression of EV miR-21-5p was significantly increased in 4 Gy-irradiated HUVECs compared with nonirradiated HUVECs. All experiments were performed with n=4. ${}^{**}P<0.01$. EV, extracellular vesicle; miR, microRNA; NC, negative control; RT-qPCR, reverse transcription-quantitative PCR.

complex MSH2-MSH3 recognizes small loops via a mechanism different from that of MSH2-MSH6, which is specific for single-base mismatches (37). This salvage pathway has been implicated in cell apoptosis, proliferation, differentiation, and inflammatory responses. MTAP catalyzes the reversible phosphorylation of 5'-methylthioadenosine, a co-product of polyamine biosynthesis (38). It has been reported that loss of MTAP in hepatocellular carcinoma cells results in cell cycle arrest (39,40). Therefore, reduced expression of MTAP may be related to the cell cycle. MTHFD1 plays a role in nucleotide synthesis and cell cycle (41,42). MTHFD1 has been reported to be related to serine metabolism, and it has been reported that when serine metabolism ceases, the expression of folate metabolism-related genes such as MTHFD1 declines and cells senescence (43). It has been reported that knockdown of ZNF704 in cancer cells halts the cell cycle and induces apoptosis (44). ZNF367 is involved in YAP signaling in carcinomas and is frequently enriched in aged brain tissue (45,46). In breast carcinomas, it negatively correlates with miR-21-5p, which has been shown to inhibit cancer cell proliferation (47).

In colon adenocarcinomas, increased expression of miR-21-5p reportedly increases cell proliferation (48). However, Li *et al* (49) reported that in chondrosarcoma, increased expression of miR-21-5p induces apoptosis by causing G0/G1 cell cycle arrest. Furthermore, Liu *et al* (50) compared kidney aging in freely-fed 3-month-old rats, 24-month-old rats, and calorie-restricted 24-month-old rats. They observed higher miR-21 expression in the freely-fed 24-month-old rats than in the calorie-restricted 24-month-old rats, suggesting that the miR-21 expression increased in the kidneys of the 24-month-old rats. This supports our results that increased miR-21 expression is associated with kidney aging (50). Mensà *et al* (51) reported that miR-21-5p

expression is increased in EVs of aging HUVECs, which are secreted by aging HUVECs as an aging signal. This suggests that miR-21-5p expression increases as cells undergo senescence (51). Thus, the accumulation of miR-21-5p contributes to the induction of cell senescence. Dellago *et al* (52) reported that overexpression of miR-21 in HUVECs causes cellular senescence, suggesting that suppression of miR-21 expression may halt the progression of cellular senescence. They also found that CDC25A, a target gene of miR-21, inhibits cell proliferation through an increase in cyclin-dependent kinase 2 (CDK2), a protein required for the transition from the G1 to S phase of the cell cycle (53). Cell cycle analysis suggests that the S phase of the cell cycle is reduced and G1 arrest occurs because of the failure of the transition from the G1 to S phase caused by decreased *CDC25A* expression. Our data also suggest that HUVECs with increased intracellular miR-21-5p and SA-β-GAL upon senescence induction are involved in the cell cycle and DNA repair by RNA-sequence enrichment analysis and cell cycle analysis. This suggests that miR-21-5p is involved in the cell cycle and DNA repair, which supports the results of our previous study.

We previously showed increased expression of mmu-miR-21a-5p in serum in cognitively impaired 58-week-old mice (28). Because the Aging mice used in the present study were even older, it suggests that the expression of mmu-miR-21a-5p persistently increases with senescence. Moreover, Accardi *et al* (54) found that plasma miR-21-5p was increased in individuals aged 51 to 99 years. They also demonstrated that passaging HUVECs induced senescence, resulting in increased intracellular miR-21-5p expression (29), which supports our results. However, they did not analyze EV miR-21-5p. Thus, our results are novel as we found miR-21-5p secretion from senescence-induced HUVECs. This suggests

that the senescent vascular endothelial cells secrete miR-21-5p, which accumulates in the blood. Based on our results and those of other groups, there is a close relationship between cognitive function, aging, and miR-21-5p expression. EV miR-21-5p may be a biomarker for the aging of vascular endothelial cells. By integrating our results with those of other researchers, we demonstrate a close relationship among miR-21-5p expression, cognitive function, and aging. In particular, miR-21-5p in EVs is a promising biomarker for vascular endothelial cell aging, potentially serving as a starting point for new studies exploring the connection between age-related cognitive decline and vascular degeneration. Future studies are required to further elucidate the functional role and mechanisms of miR-21-5p to enhance our understanding of the pathophysiology of aging. The limitation of this study is the extent to which the accumulation of endothelial cell senescence and miR-21-5p expression influence individual aging. Future research should increase the number of individual mice for detailed analysis and quantify the relationship between individual aging and the accumulation of endothelial cell senescence.

Acknowledgements

Not applicable.

Availability of data and materials

The microarray data generated in the present study may be found in the Gene Expression Omnibus database under accession number GSE274943 or at the following URL: https://www.ncbi.nlm.nih.gov/geo/query/acc.cgi?acc=GSE274943. The other data generated in the present study may be requested from the corresponding author.

Authors' contributions

KY and MC were major contributors in performing the experiments and writing the manuscript. KY and MC confirm the authenticity of all the raw data. All authors read and approved the final version of the manuscript.

Ethics approval and consent to participate

All animal experiments were performed in accordance with The Guideline for Animal Experimentation of Hirosaki University. The Animal Research Committee of Hirosaki University (approval no. AE01-2023-097-1; Hirosaki, Japan) approved and monitored the procedures. The Ethics Committee of Hirosaki University Graduate School of Health Sciences (Hirosaki, Japan) confirmed that ethical review is not required for research using commercially available, frequently used cultured cells.

Patient consent for publication

Not applicable.

Competing interests

The authors declare that they have no competing interests.

References

1. Guo J, Huang X, Dou L, Yan M, Shen T, Tang W and Li J: Aging and aging-related diseases: From molecular mechanisms to interventions and treatments. Signal Transduct Target Ther 7: 391, 2022.
2. Coppé JP, Desprez PY, Krtolica A and Campisi J: The senescence-associated secretory phenotype: The dark side of tumor suppression. Annu Rev Pathol 5: 99-118, 2010.
3. Wong PF, Tong KL, Jamal J, Khor ES, Lai SL and Mustafa MR: Senescent HUVECs-secreted exosomes trigger endothelial barrier dysfunction in young endothelial cells. EXCLI 18: 764-776, 2019.
4. Mongiardi MP, Merolle M, Fustaino V, Levi A and Falchetti ML: Gene expression profiling of hypoxic response in different models of senescent endothelial cells. Aging Clin Exp Res 33: 1993-2001, 2001.
5. Ridzuan N, Al Abbar A, Yip WK, Maqbool M and Ramasamy R: Characterization and expression of senescence marker in prolonged passages of rat bone marrow-derived mesenchymal stem cells. Stem Cells Int 2016: 8487264, 2016.
6. Xu J, Liu D, Zhao D, Jiang X, Meng X, Jiang L, Yu M, Zhang L and Jiang H: Role of low-dose radiation in senescence and aging: A beneficial perspective. Life Sci 302: 120644, 2022.
7. Tanaka Y and Takahashi A: Senescence-associated extracellular vesicle release plays a role in senescence-associated secretory phenotype (SASP) in age-associated diseases. J Biochem 169: 147-153, 2021.
8. Hallal S, Tűzesi Á, Grau GE, Buckland ME and Alxander KL: Understanding the extracellular vesicle surface for clinical molecular biology. J Extracell Vesicles 11: e12260, 2022.
9. O'Brien K, Breyne K, Ughetto S, Laurent LC and Breakefield XO: RNA delivery by extracellular vesicles in mammalian cells and its applications. Nat Rev Mol Cell Biol 21: 585-606, 2020.
10. Nowicka G: Extracellular vesicles in the diagnosis and treatment of cardiovascular disease. What's behind? What do we need to implement them into clinical practice? Int J Biochem Cell Biol 172: 106600, 2024.
11. Adduri RSR, Cai K, Velasco-Alzate K, Vasireddy R, Miller JW, de Frías SP, de Frías FP, Horimasu Y, Iwamoto H, Hattori N, et al: Plasma extracellular vesicle proteins as promising noninvasive biomarkers for diagnosis of idiopathic pulmonary fibrosis. J Extracell Biol 2: e98, 2023.
12. García-Silva S, Gallardo M and Peinado H: DNA-loaded extracellular vesicles in liquid biopsy: Tiny players with big potential? Front Cell Dev Biol 8: 622579, 2021.
13. Ekström K, Valadi H, Sjöstrand M, Malmhäll C, Bossios A, Eldh M and Lötvall J: Characterization of mRNA and microRNA in human mast cell-derived exosomes and their transfer to other mast cells and blood CD34 progenitor cells. J Extracell Vesicles 1: 18389, 2012.
14. Lagos-Quintana M, Rauhut R, Lendeckel W and Tuschl T: Identification of novel genes coding for small expressed RNAs. Science 294: 853-858, 2001.
15. Das K and Rao LV: The role of microRNAs in inflammation. Int J Mol Sci 23: 15479, 2022.
16. Nunes AD, Weigl M, Schneider A, Noureddine S, Yu L, Lahde C, Saccon TD, Mitra K, Beltran E, Grillari J, et al: miR-146a-5p modulates cellular senescence and apoptosis in visceral adipose tissue of long-lived Ames dwarf mice and in cultured preadipocytes. Geroscience 44: 503-518, 2022.
17. Suh N: MicroRNA controls of cellular senescence. BMB Rep 51: 493-499, 2018.
18. Chan JA, Krichevsky AM and Kosik KS: MicroRNA-21 is an antipoptotic factor in human glioblastoma cells. Cancer Res 65: 6029-6033, 2005.
19. Zhang X, Azhar G and Wei JY: The expression of microRNA and microRNA clusters in the aging heart. PLoS One 7: e34688, 2012.
20. Wang P, Zou F, Zhang X, Li H, Dulak A, Tomko RJ Jr, Lazo JS, Wang Z, Zhang L and Yu J: microRNA-21 negatively regulates Cdc25A and cell cycle progression in colon cancer cells. Cancer Res 69: 8157-8165, 2009.
21. Zhang Y, Liu Y, Liu H and Tang WH: Exosomes: Biogenesis, biologic function and clinical potential. Cell Biosci 9: 19, 2019.

22. Iglesias MJ, Kruse LD, Sanchez-Rivera L, Enge L, Dusart P, Hong MG, Uhlén M, Renné T, Schwenk JM, Bergstrom G, et al: Identification of endothelial proteins in plasma associated with cardiovascular risk factors. Arterioscler Thromb Vasc Biol 41: 2990-3004, 2021.
23. Berezin AE and Berezin AA: Extracellular endothelial cell-derived vesicles: Emerging role in cardiac and vascular remodeling in heart failure. Front Cardiovasc Med 15: 47, 2020.
24. Casella G, Munk R, Kim KM, Piao Y, De S, Abdelmohsen K and Gorospe M: Transcriptome signature of cellular senescence. Nucleic Acids Res 47: 7294-7305, 2019.
25. Chiba M, Uehara H, Niiyama I, Kuwata H and Monzen S: Changes in miRNA expressions in the injured small intestine of mice following high-dose radiation exposure. Mol Med Rep 21: 2452-2458, 2020.
26. Yamamoto K and Chiba M: Examination and comparison of the RNA extraction methods using mouse serum. Biomed Rep 20: 51, 2024.
27. Ritchie ME, Phipson B, Wu D, Hu Y, Law CW, Shi W and Smyth GK: limma powers differential expression analyses for RNA-sequencing and microarray studies. Nucleic Acids Res 43: e47, 2015.
28. Yamamoto K, Miyano K, Fujita M, Kurata W, Ohta H, Matsumoto K and Chiba M: Changes in cognitive ability and serum microRNA levels during aging in mice. Exp Ther Med 27: 120, 2024.
29. Bouten RM, Dalgard CL, Soltis AR, Slaven JE and Day RM: Transcriptomic profiling and pathway analysis of cultured human lung microvascular endothelial cells following ionizing radiation exposure. Sci Rep 11: 24214, 2021.
30. Livak KJ and Schmittgen TD: Analysis of relative gene expression data using real-time quantitative PCR and the 2(-Delta Delta C(T)) method. Methods 25: 402-408, 2001.
31. Chen S, Zhou Y, Chen Y and Gu J: fastp: An ultra-fast all-in-one FASTQ preprocessor. Bioinformatics 34: i884-i890, 2018.
32. Patro R, Duggal G, Love MI, Irizarry RA and Kingsford C: Salmon provides fast and bias-aware quantification of transcript expression. Nat Methods 14: 417-419, 2017.
33. Soneson C, Love MI and Robinson MD: Differential analyses for RNA-seq: Transcript-level estimates improve gene-level inferences. F1000Res 4: 1521, 2015.
34. Chen Y, Lun AT and Smyth GK: From reads to genes to pathways: Differential expression analysis of RNA-Seq experiments using Rsubread and the edgeR quasi-likelihood pipeline. F1000Res 5: 1438, 2016.
35. Yu G, Wang LG, Han Y and He QY: clusterProfiler: An R package for comparing biological themes among gene clusters. OMICS 16: 284-287, 2012.
36. Yu G and He QY: ReactomePA: An R/Bioconductor package for reactome pathway analysis and visualization. Mol Biosyst 12: 477-479, 2016.
37. Edelbrock MA, Kaliyaperumal S and Williams KJ: Structural, molecular and cellular functions of MSH2 and MSH6 during DNA mismatch repair, damage signaling and other noncanonical activities. Mutat Res 743: 53-66, 2013.
38. Fan N, Zhang Y and Zou S: Methylthioadenosine phosphorylase deficiency in tumors: A compelling therapeutic target. Front Cell Dev Biol 5: 1173356, 2023.
39. Marjon K, Cameron MJ, Quang P, Clasquin MF, Mandley E, Kunii K, McVay M, Choe S, Kernytsky A, Gross S, et al: MTAP deletions in cancer create vulnerability to targeting of the MAT2A/PRMT5/RIOK1 axis. Cell Rep 15: 574-587, 2016
40. Kryukov GV, Wilson FH, Ruth JR, Paulk J, Tsherniak A, Marlow SE, Vazquez F, Weir BA, Fitzgerald ME, Tanaka M, et al: MTAP deletion confers enhanced dependency on the PRMT5 arginine methyltransferase in cancer cells. Science 351: 1214-1218, 2016.
41. Galbiatti AL, da Silva LM, Ruiz-Cintra MT, Raposo LS, Maníglia JV, Pavarino ÉC and Goloni-Bertollo EM: Association between 11 genetic polymorphisms in folate-metabolising genes and head and neck cancer risk. Eur J Cancer 48: 1525-1531, 2012.
42. He D, Yu Z, Liu S, Dai H, Xu Q and Li F: Methylenetetrahydrofolate dehydrogenase 1 (MTHFD1) is underexpressed in clear cell renal cell carcinoma tissue and transfection and overexpression in Caki-1 cells inhibits cell proliferation and increases apoptosis. Med Sci Monit 21: 8391-8400, 2018.
43. Zhou S, Cui J and Shi Y: Serine metabolism regulates the replicative senescence of human dental pulp cells through histone methylation. Curr Issues Mol Biol 24: 2856-2870, 2024.
44. Luo J, Li H, Xiu J, Zeng J, Feng Z, Zhao H, Li Y and Wei W: Elevated ZNF704 expression is associated with poor prognosis of uveal melanoma and promotes cancer cell growth by regulating AKT/mTOR signaling. Biomark Res 10: 38, 2023
45. Lei T, Gao Y, Duan Y, Cui C, Zhang L and Si M: Inhibition of zinc finger protein 367 exerts a tumor suppressive role in colorectal cancer by affecting the activation of oncogenic YAP1 signaling. Environ Toxicol 36: 2278-2290, 2021.
46. Baumgart M, Groth M, Priebe S, Savino A, Testa G, Dix A, Ripa R, Spallotta F, Gaetano C, Ori M, et al: RNA-seq of the aging brain in the short-lived fish N. furzeri-conserved pathways and novel genes associated with neurogenesis. Aging Cell 13: 965-974, 2014.
47. Du L, Tao X and Shen X: Human umbilical cord mesenchymal stem cell-derived exosomes inhibit migration and invasion of breast cancer cells via miR-21-5p/ZNF367 pathway. Breast Cancer 28: 829-837, 2021.
48. Yu W, Zhu K, Wang Y, Yu H and Guo J: Overexpression of miR-21-5p promotes proliferation and invasion of colon adenocarcinoma cells through targeting CHL1. Mol Med 24: 36, 2018.
49. Li G, Yang Y, Xu S, He M and Zhang Z: mir-21-5p inhibits the progression of human chondrosarcoma by regulating CCR7/STAT3/NF-κB pathway. Connect Tissue Res 62: 313-324, 2021.
50. Liu JR, Cai GY, Ning YC, Wang JC, Lv Y, Guo YN, Fu B, Hong Q, Sun XF and Chen XM: Caloric restriction alleviates aging-related fibrosis of kidney through downregulation of miR-21 in extracellular vesicles. Aging 27: 18052-18072, 2020.
51. Mensà E, Guescini M, Giuliani A, Bacalini MG, Ramini D, Corleone G, Ferracin M, Fulgenzi G, Graciotti L, Prattichizzo F, et al: Small extracellular vesicles deliver miR-21 and miR-217 as pro-senescence effectors to endothelial cells. J Extracell Ves 18: 1725285, 2020.
52. Dellago H, Preschitz-Kammerhofer B, Terlecki-Zaniewicz L, Schreiner C, Fortschegger K, Chang MW, Hackl M, Monteforte R, Kühnel H, Schosserer M, et al: High levels of oncomiR-21 contribute to the senescence-induced growth arrest in normal human cells and its knock-down increases the replicative lifespan. Aging Cell 12: 446-458, 2013.
53. Donzelli M and Draetta GF: Regulating mammalian checkpoints through Cdc25 inactivation. EMBO Rep 4: 671-677, 2003.
54. Accardi G, Bono F, Cammarata G, Aiello A, Herrero MT, Alessandro R, Augello G, Carru C, Colomba P, Costa MA, et al: miR-126-3p and miR-21-5p as hallmarks of bio-positive ageing; correlation analysis and machine learning prediction in young to ultra-centenarian Sicilian population. Cells 11: 1505, 2022.